Brushless traction PM Machines using commercial drive technology, part I: Design methodology and motor design

Brushless Traction PM Machines Using Commercial Drive Technology, Part I: Design Methodology and Motor Design

Evgeny V. Kazmin, Elena A. Lomonova, Johannes J.H. Paulides
Department of Electrical Engineering, Eindhoven University of Technology, The Netherlands
Email: e.lomonova@tue.nl

***Abstract* - A concept design approach for the brushless PM traction motor, which has crucial constraints on volume envelope and on the drive, is presented. The considered motor drive is the three-phase DC/AC converter, which is commercially available on the modern market of the standard variable frequency drives. The features of the motor design procedure, which are imposed by the peculiarities of an automotive application and commercial drive technology, are given. The developed concept design procedure is applied to design of an 80-kW in-wheel hub motor of the hybrid truck that achieves wide constant power speed range. In this paper, which is one of the series of two, the description of the basic design steps and the concept design on the example of the surface-mounted PM (SPM) motor with concentrated armature winding are presented. The concept design of the motor includes electromagnetic, thermal and hydraulic analyses, which are conducted to define the motor performances and thermal conditions.**

***Index Terms* - Brushless motor, permanent magnets, field weakening, concentrated winding, fractional slot, commercial vehicle.**

I. INTRODUCTION

During the past eighty years or so, we have seen a tremendous growth in the use of electric machines in the industrial world and autonomous more electrical solutions (automotive, aircraft, marine, etc.). The principal workhorse of this motor industry has been the three-phase induction motor; also the DC shunt motor was a significant ”prime mover”. Nowadays, AC drives ranging from 1 kW 100kW have become the dominant technology in nearly all sectors of the industrial market largely supplanting DC drives. Design sophistication of the AC drives has reached the level where, in lower power ranges, the drives, produced by different manufacturers, are nearly identical. Brushless AC permanent magnet (PM) machines are also increasingly used in higher power (10’s kW) applications, where motor manufacturers attempt to utilize commercially available AC drive technology. Assuming that cost, efficiency, size, and low maintenance are the key issues in drive system selection, brushless motors and drives have employed a “heritage of standard” applications. However, one of the drawbacks of this industrial vision is that the most power electronics solutions have frequency limitations and are grid supplied.

As an example of the hybrid automotive application, which requires competitive powertrain technologies, heavy trucks could be considered with a total weight more than 7.5 tones. In order to minimize the truck production and maintenance costs, commercial drives should be used. The key features of this drives are given in section II.

The purpose of this paper is to present a design approach for the brushless PM traction motors, which are violently constrained by volume envelope and imposed to use abovementioned drives. This approach includes electromagnetic, thermal and hydraulic analyses for the development of the concept motor design, which should figure out the maximum achievable performance indexes without full optimization of the motor construction.

The correlation between the motor parameter values required for a 4.5:1 field weakening performance and the main design rules for such machines using conventional electronics are the subject of this paper.

II. COMMERCIAL DRIVE TECHNOLOGY

In Fig. 1 the required torque and output power versus speed characteristics are shown. The continuous operation mode is the nominal (rated) regime with the torque and the output power curves, as shown in Fig. 1. Peak torque and output power motor performance are required for discontinuous operation during one minute.

The motor should be sized for the so-called base speed field-weakening (FW) point, which is near the knee of the curves (see Fig. 1). The FW base speed point has the following specified parameters: 1000 rpm, 80 kW, 750 Nm.

It should be noted also that the motor is being designed with an indirect cooling system such as water-jacket filled by a water-glycol liquid. The water-jacket is placed in the stator housing (interior rotor) or the stator hub (exterior rotor).

Almost all of the contemporary drives have a maximum output frequency of 300 Hz that applies the main constraint on the motor design. This constraint is a maximum number of poles, which is limited by the maximum value of the drive frequency. At 300 Hz and 4500 rpm the maximum number of pole pairs is equal to 4. It is well known that the output power

of the electrical machine is proportional to the square of airgap diameter [1]. In order to maximize the airgap diameter at limited outer diameter the number of poles should be as higher as possible.

Among other motor constraints which are imposed by the drive one can be indicated the terminal voltage and apparent power, which are within standard series inherent to the grid parameters.

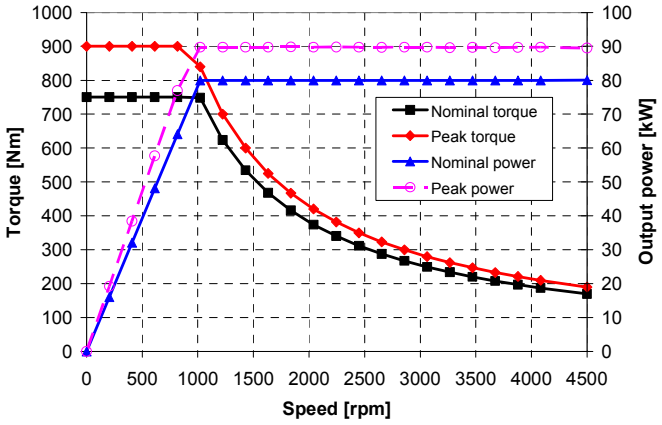

Fig. 1. Output power and torque vs. speed characteristics

All abovementioned design constraints have a very large impact on the possible motor type and configuration. In section V partially and in the second part of this paper (Part II, this issue) the proofs of the selection of appropriate machine configuration for the given application, which uses commercial drive technology, are given.

III. Field-Weakening Operation of PM Machines

Electrical motors for automotive applications generally require operation with constant torque up to a speed ω_1, which is at knee point and constant power up to a top speed, ω_m, as shown in Fig. 2. The ratio of ω_m to ω_1 is normally referred to as the speed range.

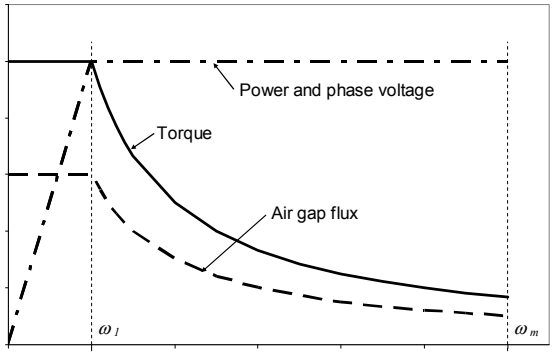

Fig. 2. Motor performances at flux-weakening operation

In order to extend the speed range of the PM synchronous machines field-weakening control is used [1], [2]. The basic idea of field-weakening control is to use additional armature current to create a magnetic field that opposes or weakens the airgap flux so that the motor's back-emf can be kept constant.

Omitting the details of the FW operation which are widely discussed in many literature sources, it is possible to analyze the output power, P^*_{out}, versus speed characteristics. In Fig. 3, 4 these P^*_{out} versus speed characteristics of SPM motor for the fixed back-emf, E_0, and d-axis armature reactance, X^*_d, respectively, are shown. In these graphs the FW coefficient, k_{FW}, is defined as follows:

$$k_{FW} = \frac{E_0}{X^*_d}. \qquad (1)$$

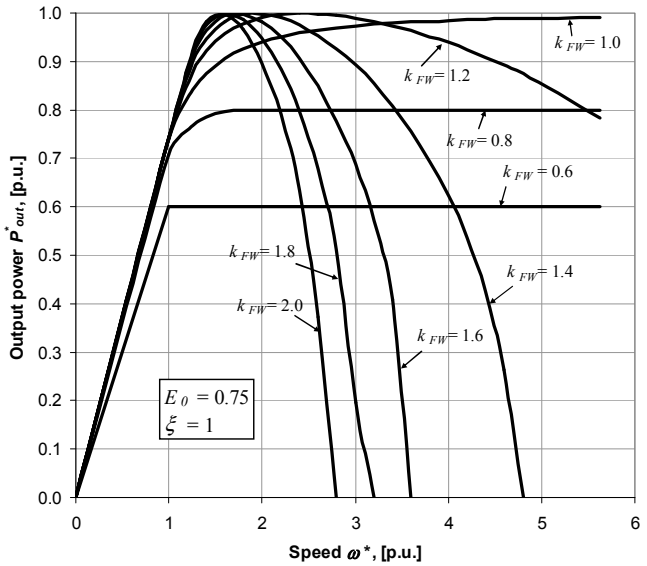

Fig. 3. Output power vs. speed characteristics at fixed E_0

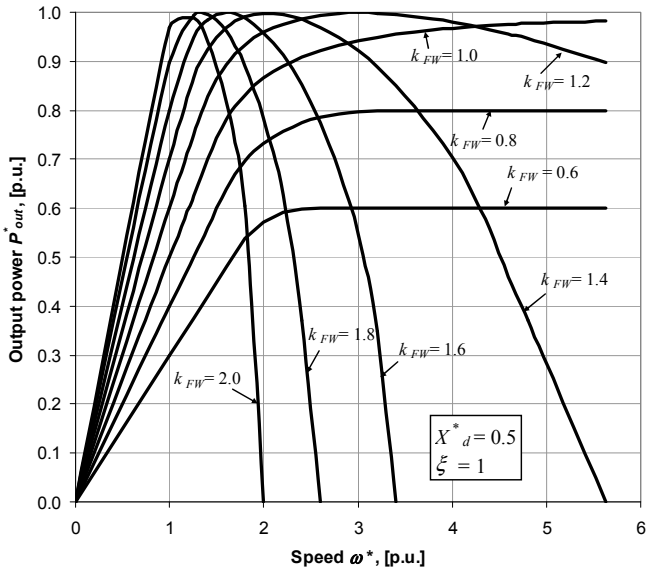

Fig. 4. Output power vs. speed characteristics at fixed X^*_d

The coefficient k_{FW} is a characteristic current in per unit system that defines the minimum possible armature current, which can provide optimal field-weakening in the PM machines [3]. In case of the SPM motor the optimal FW is achieved at $k_{FW} = 1$, when the rated armature current is equal to the characteristic current.

At fixed E_0 decreasing of the k_{FW} increases the X^*_d, and

gives a better FW performance, as shown in Fig. 3. However, the output power, P^*_{out}, and, therefore, the power factor of the motor are decreased. So, the motor requires a larger inverter VA-capability.

At fixed X^*_d increasing of the k_{FW} gives rise to the E_0, and correspondingly produces a better FW performance at k_{FW} = 0.8 – 1.2, as shown in Fig. 4. At higher values of the k_{FW} >1.2 the output power at base speed is increased significantly, but the FW operation is drastically degraded.

Thus, the high output power of the motor and its capability to operate over the wide constant power speed range (CPSR) are in a contradiction. The wide CPSR and high output power could be achieved at k_{FW} = 0.8 – 1.2, as shown in Fig. 3 and Fig. 4.

As it is well-known, in order to increase P^*_{out} the airgap flux density and electrical loading of the motor should be increased. At the same time, as it was mentioned above, it is necessary to have k_{FW} near the unity. By means of the proper design of the PM motor it is possible to satisfy the both contradictory requirements.

IV. PM TRACTION MOTOR DESIGN METHODOLOGY

A. Considered types of the PM motors

The design methodology is developed for the analysis of the pre-selected PM motor configurations. The considered PM motor types are shown in Fig. 5. The PM motors are classified in three different categories. The first of them is the rotor type, which defines the non-salient surface-mounted PM (SPM) and salient interior PM (IPM) rotors. It should be noticed that, although some authors referred an inset type of the rotor to the SPM rotors [4], in this paper it is designated as the IPM rotor because of the saliency. The second category is the rotor arrangement that defines the position of the rotor relatively to the stator (Fig. 5). The last motor category is the type of the armature winding. The concentrated and distributed armature windings have been studied (Fig. 5). The details of the considered motor configurations are given in the Part II of this paper.

While many authors [4], [5] prefer the inset or even interior PM configuration, which is not considered as an objective of this paper. PM machines for the FW operation over wide CPSR, with required high specific power and, therefore, high level of iron saturation can eliminate the attractive benefits of these machines. Selection of the most appropriate motor configuration among considered types is highly challenging task that could not be done without detailed electromagnetic and thermal designs. In next sections the main topics of the developed design methodology are given.

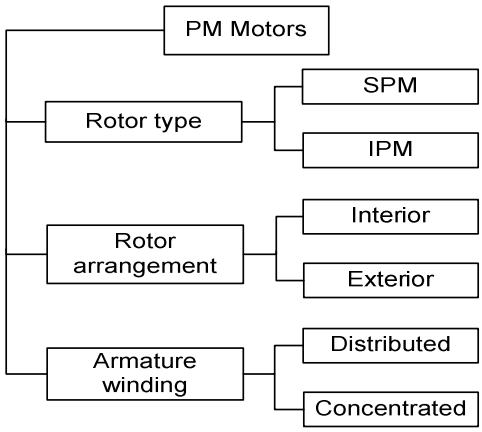

* - Only inset type of SPM rotor with (or without) saturation bridges is considered

Fig. 5. PM motor configurations

B. Algorithm of PM motor design approach

The objective of this paper is to provide only a preliminary design of the motor, which should show the most appropriate motor type, its basic dimensions and maximum achievable performance characteristics. This design should satisfy the design requirements, including given sizes and performance characteristics.

A flow-chart of the developed motor design strategy is shown in Fig. 6 [6]. At the first stage the analytical design is conducted (see Fig. 6). At this stage the motor could be initially sized with approximately calculated parameters and performance indexes, assuming the infinite permeabilities of the stator and rotor cores.

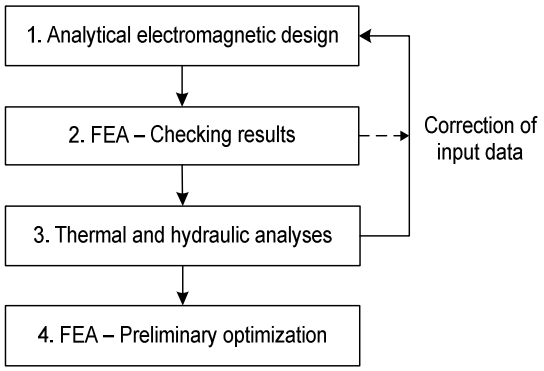

Fig. 6: A flow-chart of the motor concept design methodology

Further, at the second stage the base speed operation mode of the initially sized motor is calculated by means of the transient finite element (FE) analysis, which includes iron saturation and rotor movement. In the case when the motor performance indexes calculated by analytical and FE methods are not matched with required accuracy, the analytical analysis is repeated with an employment of the correction factors, which take into account iron saturation. When the accuracy of the analytical model is reached, the third stage is initialized. At this stage the thermal and hydraulic analyses are carried

out. The maximum possible electric loading, current density and airgap flux density of the motor could be defined at this design level.

Once the performance and temperature conditions of the designed motor satisfy all design requirements, it is possible to make a preliminary optimization of the motor with the aim to minimize a torque ripple and magnet eddy current losses (see the fourth phase of flow-chart in Fig. 6).

C. Analytical model

A flow-chart of analytical design method is shown in Fig. 7. It is based on the phasor diagram analysis of the base speed and other field-weakening operation points and subsequent correction using FE analysis.

The basic assumptions of the analytical model are the following:

1) Iron saturation is neglected;

2) Stator and rotor iron losses are neglected;

3) Magnet eddy current losses are neglected;

4) Due to negligible saliency of the SPM motor design the equivalent airgaps along *d*- and *q*-axis are assumed to be equal. Thus, the synchronous reactances along those axes are also equal.

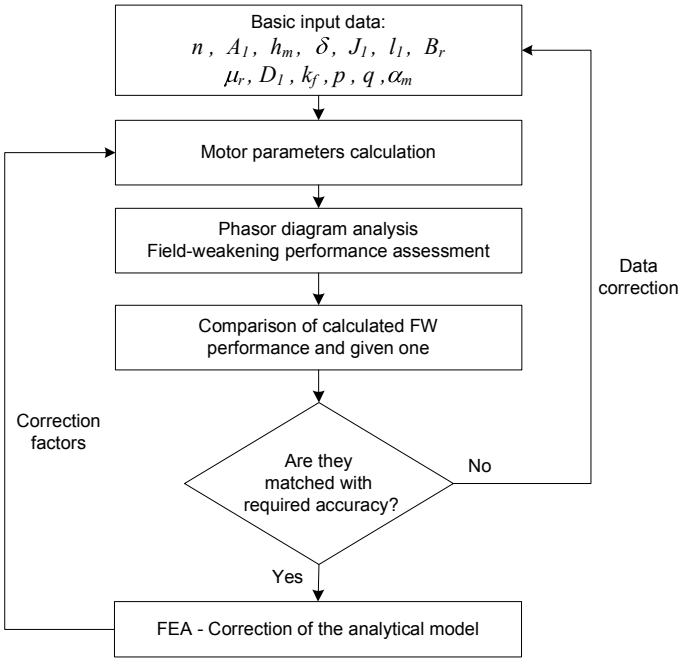

Fig. 7: A flow-chart of the analytical method

In Fig. 7 the following symbols are used:
n – rotor speed [rpm]; A_1 – armature electrical loading [A/m]; h_m – magnet height [m]; δ – airgap height [m]; J_1 – armature current density [A/mm^2]; l_1 - stator stack length [m]; B_r and μ_r – residual flux density and recoil permeability of the magnet [T], [p.u.], respectively; D_1 – stator bore diameter [m]; k_f – net slot fill factor (without area of the wedge region); p – number of pole pairs; q – number of slots per pole and phase; α_m – magnet span angle [electrical degrees];

This design approach is implemented as a set of analytical formulas which are described in synchronous motors design books [1], [7]. The only difference from those methods is the calculation of the armature mutual and differential leakage reactances (also called airgap armature reactances) of the concentrated winding machine with fractional number of slots per pole and phase. In such machines these parameters are drastically affected by the stator slotted structure and reach harmonic distortion of the winding. The conventional methods [1], [7] do not allow properly accounting these phenomena. The so-called "*slot impact factors"* on a harmonic of the airgap flux density has been used in order to resolve such a problem [8]. These factors are calculated by using tooth-contour method (TCM) [9]. This method is based on representation of the total magnetic field in the air-gap region of an electric machine as the sum of local magnetic fields of the particular elements of the electric machine magnetic system, the so-called tooth contours. One of the main assumptions of this method is that the real circumferential shape of the airgap is replaced by the rectangular one and the rotor core is considered as a smooth surface, introducing a Carter's factor. In this method an airgap flux density is estimated separately for each harmonic component by the calculation of the relative specific permeances of the tooth contours with taking into account stator slotted structure. These permeances are calculated by means of the Carter's conformal mapping and further are resolved on the harmonic components. By using these permeances the harmonic components of the airgap flux density could be defined and consequently mutual armature reactances caused by these harmonics could be calculated as well. It makes possible to separate fundamental harmonic, which produces the main torque, from the high order harmonics and subharmonics, which have a larger pole pitch then that of the fundamental one. The high order harmonics and subharmonics of the airgap armature reactance are recognized as differential leakage reactance of the machine. That allows calculating abovementioned parameters analytically with the accuracy comparable with a FE analysis.

This method makes it possible to use classical analytical design techniques, including the *d-q* phasor diagrams, in the same manner as for the conventional distributed winding machines. Computation algorithm of the method (Fig. 7) is done by means of an analytical tool using the Excel workbook functions and programming on visual basic language as well [6]. The main advantage of this tool is a very fast assessment of the motor FW performance. By using a short list of input data (Fig. 7) and relatively simple equations it is possible to define the main motor dimensions, calculate the rated performance and select the best design parameters of the motor configuration: pole and stator teeth numbers, magnet dimensions and electromagnetic loads.

D. Description of the machine sizing procedure

Many of the sizing procedure steps for the considered motor types are the same used for any other types of electrical

machines [1]. However, several steps of the sizing process are the different ones, which are briefly discussed in this section.

1) Stator slots

By using the input data which is presented in Fig. 7 it is possible to calculate the necessary dimensions of the stator slots. For instance, this approach could be illustrated by means of the example of the interior rotor machine with the concentrated winding. The stator slot configuration of this machine is shown in Fig. 8.

The following stator configuration dimensions should be predefined in advance (Fig. 8): h_{so}, b_{so} – slot opening width and height [m]; h_w – wedge height [m]; k_{bs_tz} – slot width to slot pitch ratio. These dimensions could be selected as the fixed parameters for the set of machine design solutions. Usually, they are selected on the basis of the design experience of the similar machine types and could be changed during design process.

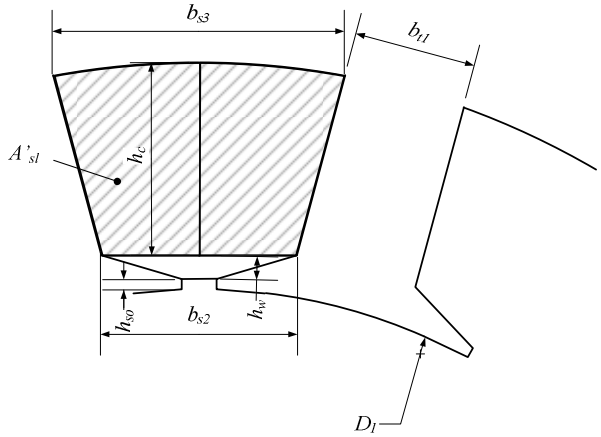

Fig. 8: Stator slot configuration for the interior rotor PM machine with concentrated winding

Omitting an intermediate expressions the following system of equations, which define the basic sizes of the slots, could be written as:

$$\begin{aligned} &A'_{sl} = \frac{1}{2}\cdot(b_{s2}+b_{s3})\cdot h_c; \\ &\frac{\pi\cdot(D_1+k_{I/O}\cdot(h_w+h_{so}+h_c))}{Z} = b_{s3}+b_{t1}, \end{aligned} \quad (2)$$

where A'_{sl} – area of the slot that fulfilled by the coils [m^2]; $k_{I/O}$ – coefficient that defines machine arrangement (for inner rotor $k_{I/O}$ = 1; for outer rotor $k_{I/O}$ = – 1); b_{t1} – tooth width [m]; b_{s2} and b_{s3} – slot widths at the top and bottom of the coil, respectively [m]; h_c – coils height [m]; $Z=2pqm$ – number of stator slots.

The area A'_{sl} is expressed as:

$$A'_{sl} = \frac{A_1\cdot t_{z2}}{J_1\cdot k_f}, \quad (3)$$

where A_1 – armature electrical loading (rms) [A/m]; t_{z2} – stator slot pitch at coil top [m].

The stator slot pitch at coil top, t_{z2}, is defined as follows:

$$t_{z2} = \frac{\pi\cdot(D_1+k_{I/O}\cdot 2\cdot(h_w+h_{so}))}{Z}, \quad (4)$$

where D_1 – stator bore diameter [m] (Fig. 8).

The tooth width, b_{t1}, is defined as:

$$b_{t1} = \frac{\pi\cdot D_1}{Z}\cdot(1-k_{bs\_tz}). \quad (5)$$

The slot width at coil top is expressed as:

$$b_{s2} = \frac{\pi\cdot(D_1+k_{I/O}\cdot 2\cdot(h_w+h_{so}))}{Z} - b_{t1}. \quad (6)$$

In (2) the b_{s3} and the h_c are unknown. By solving the system (2) the slot width, b_{s3}, could be defined as:

$$b_{s3} = \frac{1}{2}\cdot\left(\pi\cdot t_{z2} - b_{s2} - b_{t1} + \sqrt{A+B+C}\right), \quad (7)$$

where

$$A = {b_{s2}}^2 + 2\cdot b_{s2}\cdot t_{z2}, \quad (8)$$

$$B = \pi^2\cdot {t_{z2}}^2 - 2\cdot b_{s2}\cdot b_{t1}, \quad (9)$$

$$C = {b_{t1}}^2 - 2\cdot t_{z2}\cdot b_{t1} + 16\cdot\pi\cdot k_{I/O}\cdot A'_{sl}\cdot\frac{1}{Z}. \quad (10)$$

The stator coil height, h_c, then yields:

$$h_c = \frac{A'_{sl}}{b_{av}}, \quad (11)$$

where

$$b_{av} = \frac{1}{2}\cdot(b_{s2}+b_{s3}). \quad (12)$$

The calculation of the back-iron height and other dimensions of the stator is conducted by the conventional formulas which are well documented in the literature [1].

2) Rotor

Since the PM characteristics in many cases are given by a customer, the magnet remanence, B_r, and recoil permeability, μ_r, are fixed. The magnet height, h_m, is used as the common input data (Fig. 7), and magnet span angle, α_m, is selected during design procedure (Fig. 6). By the proper selection of the PM sizes (and electrical loading A_1, as well) it is possible to obtain required output power at base speed and to keep the coefficient of the FW, k_{FW}, near an optimal level, as it was discussed in section III.

V. Draft Design of the SPM Motor with Concentrated Winding

As it is mentioned in the section II the number of pole pairs should be as higher as possible, but not more than 4. The concentrated winding with a number of pole pairs equal to 4 and number of stator slots equal to 9 has been selected as the most suitable CW among the others [10]. This winding has the highest winding factor, k_{wp} = 0.945.

After several iterations within the developed algorithm for the motor design the intermediate SPM concentrated winding motor with interior rotor has been achieved. The motor cross-section drawing of the motor is shown in Fig. 9 and the basic dimensions and performance data are presented in Table I and Table II.

The machine configuration has the number of slots per pole and phase q=3/8 and only one spatial period per whole circumference (see Fig. 9). That circumstance leads to

necessity to model by FE method an entire machine without a possibility to exploit symmetry.

FE analysis is conducted by means of FLUX 2D software [11]. The main assumption of the developed FE model is that the armature current contains only fundamental harmonic and the armature coils are fed by this current. In Table II the main results derived from this model are presented and compared with the results of the analytical model. The calculated performance data of the both methods are in the good agreement, considering rather simplicity of the developed analytical model. The main differences in the results are in the phase voltage and output power. It could be explained by the iron saturation effect, especially of stator and rotor back irons and also by the stator tooth tips. For the illustration of this a vector sum of the flux density and flux lines are shown in Fig. 10.

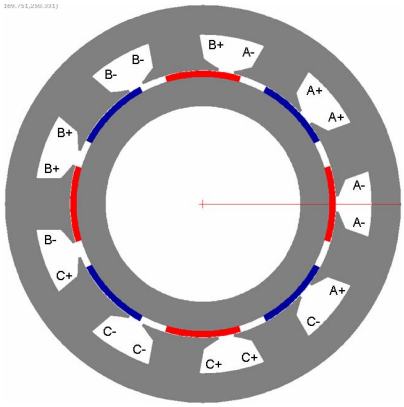

Fig. 9: Cross-section of the SPM interior rotor motor with concentrated winding

TABLE I
BASIC MOTOR GEOMETRY AND WINDING DATA

Description	Symbol	Unit	Value
Number of pole pairs	p	-	4
Number of slots	Z	-	9
Number of slot per pole per phase	q	-	3/8
Stator outer diameter	D_{OD}	mm	501.3
Stator bore diameter	D_1	mm	338
Stack length	l_1	mm	100
Airgap height	δ	mm	1
Magnet height	h_m	mm	7.5
Magnet span angle	α_m	el.deg.	132
Magnet remanence	B_r	T	1.175
Magnet recoil permeability	μ_r	-	1.05
Number of turns per branch	w_1	-	78
Net slot fill factor	k_f	-	0.65

As a result of such saturation the back-emf of the motor calculated at open circuit magnetic state differs from that which calculated at rated load one. Due to high armature reaction flux, that oriented at base speed along q-axis and is not weaken by the magnet flux, the magnetic core of the machine becomes higher saturated. Although in less rated PM synchronous motors this does not occur. However, it is conventional to define the back-emf exactly at open circuit conditions. The back-emfs, which were calculated in that way by analytical method and FEA, are in quite good agreement (see Table II).

TABLE II
CALCULATED MOTOR PERFORMANCES AT BASE SPEED OPERATION MODE

Description	Symbol	Unit	Value	
			Analytical tool	FEA
Speed	n	rpm	800	800
Electrical loading	A_1	A/m	56000	56000
Current density	J_1	A/mm^2	5.0	5.0
Phase current	I_1	Arms	138.3	138.3
Phase voltage	V_1	Vrms	219.5	208.2
Output power	P_{out}	kW	68.9	60.9
Shaft torque	T_{out}	Nm	823	726
Airgap peak flux density at open circuit conditions	$B_{\delta m}$	T	0.947	0.984
Back-emf	E_q	Vrms	162.6	160.7
d-axis synchronous inductance	L_d	mH	3.093	3.094
Saliency ratio	ξ	-	1.0	1.0
Ratio E_0/X^*_d	-	-	1.13	1.12
Peak-peak cogging torque	ΔT_{cog}	%	-	1.2
Peak-peak torque ripple	ΔT_{rip}	%	-	5.2
Efficiency (electric)	η	%	97.5	97.4

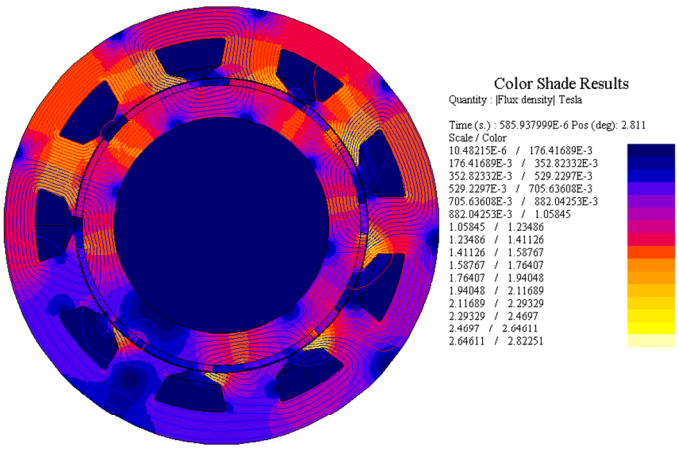

Fig. 10: Color map of flux density vector sum and 2D flux lines for arbitrary instant of time

The distribution of the airgap flux density along whole motor circumference is shown in Fig. 11. It could be seen that the peak airgap flux densities at the open circuit is about of 0.984 T, while at the rated load – 1.2-1.6 T.

The phase current, back-emf and phase voltage are shown on Fig. 12. It can be observed that phase back-emf is quite close to sine and slightly influenced by the iron saturation (some flattening of the waveform). In contrast, the phase voltage waveform is significantly distorted (see Fig. 12) that is caused, as it was mentioned before, by the saturation of the machine.

In Fig. 16 the required, analytically and FEA calculated

output power vs. speed characteristics are shown. It can be seen that required constant power speed range is achieved, but power level is not satisfy design requirements. The possibility to increase of the output power should be investigated by means of the thermal analysis, basic results of which are given further.

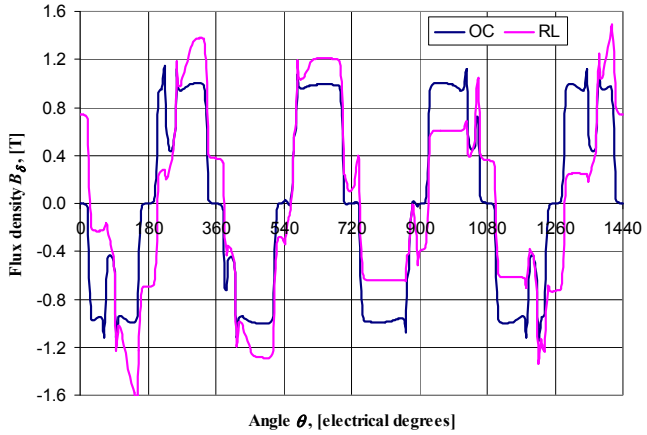

Fig. 11: Airgap flux density distribution along whole motor circumference at open circuit (OC) and rated load (RL) conditions at base speed calculated by FEA

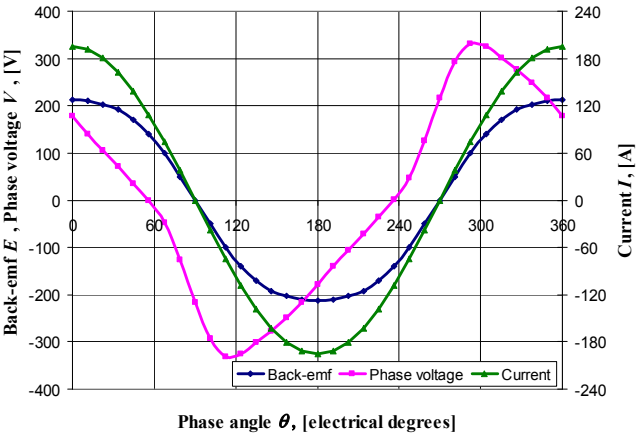

Fig. 12: Phase back-emf, voltage and current waveforms calculated by FEA

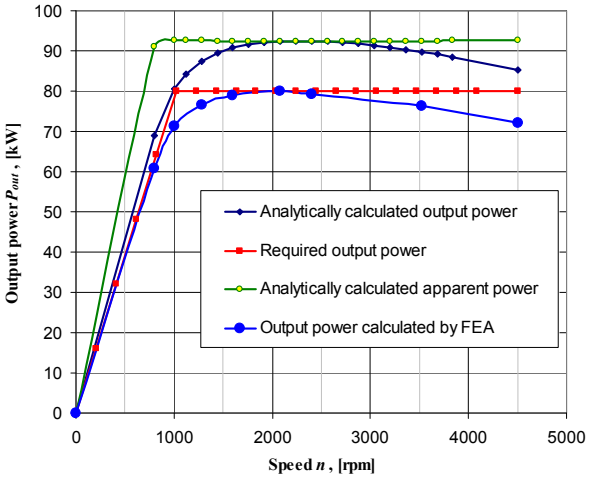

Fig. 13: Output power versus speed characteristics

The fact that the calculated power vs. speed envelope is in a quite good agreement with the required one is consistent with achieved near optimal FW coefficient k_{FW}=1.12 (see Table II). This correlates with the analysis of the FW operation of the SPM machine that has been given in section III.

Thermal analysis is done by Motor-CAD software [12]. In Fig. 14 the longitudinal section of the motor with a water jacket (WJ) in stator housing is shown. The hydraulic analysis is done by means of analytical method, description of which goes beyond the objectives of this paper and is given in [6]. The results of thermal and hydraulic analyses are presented in Table III.

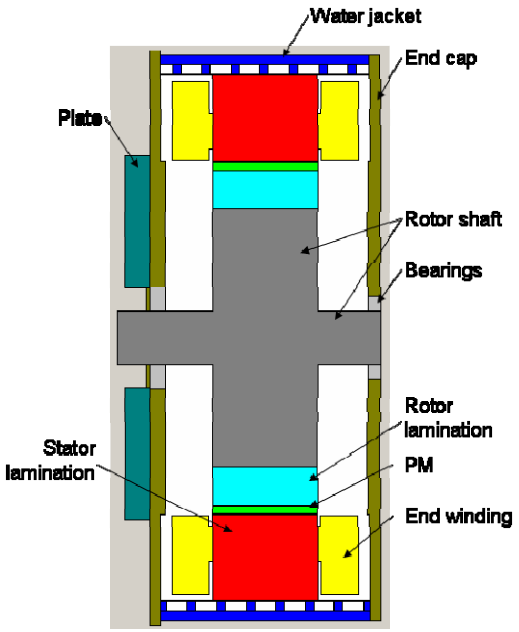

Fig. 14: Axial cross-section of the motor

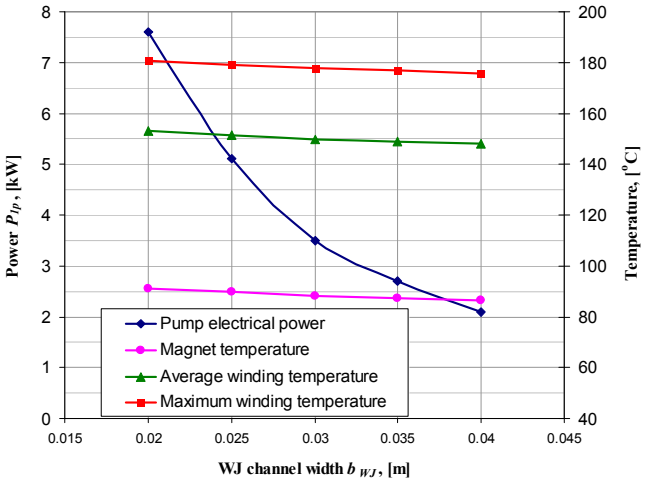

Fig. 15: Axial cross-section of the motor

The required input power of the pump, P_{1p}, which is needed to provide a circulation of the coolant in the WJ with required velocity, is equal to 7.6 kW that is almost 10% of the motor output power (Table II). In order to reduce the P_{1p} a channel width of the WJ, b_{WJ}, should be increased. At the same time with increasing of the b_{WJ} the fluid volume flow rate, Q_f, should be also increased to keep the fluid velocity, v_f, at the constant level. The constant level of the v_f is needed to keep the approximately same cooling capability of the WJ and to have the same laminar fluid of the coolant. The impact of the b_{WJ} on the electrical power of the pump, P_{1p}, and the motor temperatures is shown in Fig. 15.

TABLE III
BASIC RESULTS OF THE THERMAL AND HYDRAULIC ANALYS

Description	Symbol	Unit	Value
Ambient temperature	T_0	ºC	40
Average copper temperature	T_{Cuav}	ºC	153
Maximum copper temperature	T_{Cumax}	ºC	181
End winding copper temperature	T_{ew}	ºC	134
Stator teeth temperature	T_{st}	ºC	85
Stator back iron temperature	T_{sby}	ºC	77
Magnet temperature	T_{PM}	ºC	91
Rotor lamination temperature	T_{rby}	ºC	92
WJ channel width	b_{WJ}	mm	20
WJ channel height	h_{WJ}	mm	9.5
Number of parallel flow paths	a_{WJ}	-	2
Coolant type	-	-	Water-glycol
Coolant inlet temperature	T_{in}	ºC	40
Fluid velocity	v_f	m/s	0.42
Fluid volume flow rate	Q_f	m^3/s	0.00016
Friction losses in the WJ	F_{frWJ}	kW	3.8
Efficiency of the pump	η_p	p.u.	0.5
Required input power of the pump	P_{1p}	kW	7.6

Increasing the b_{WJ} two times gives reduction of the required electrical power of the pump by 3.6 times (from 7.6 kW up to 2.1 kW). Besides reducing P_{1p} the motor temperatures are also slightly decreased, as shown in Fig. 15. It means that it is possible to achieve an acceptable level of P_{1p} by means of a proper selection of the WJ dimensions or even by changing of the channel configuration. The design of the WJ is not an objective of this paper.

VI. CONCLUSION

A main contribution of this paper is the developed and verified (by FE method) design methodology of the inverter driven PM synchronous motor for traction application. This method includes the analytical and FEM electromagnetic analyses, thermal and hydraulic designs.

The eight-pole SPM motor with the concentrated armature winding has been designed using this methodology. The motor performance does not fully satisfy the design requirements and specifically the output power versus speed characteristics (Fig. 13). The main design constraint which mostly influences the motor parameters and performance indexes is the maximum output frequency of the inverter. For the designed motor the constant power speed range of 1000 - 4500 rpm and maximum inverter frequency of 300 Hz the maximum possible number of rotor pole pairs is not higher than four. As it is well known, the motor back-iron sizes and other dimensions of the core are dependent on the airgap flux per each pole, which is inversely proportional to the number of rotor poles. In addition to limitation of the number of poles the electrical loading of the designed motor has been selected at a quite high level to maximize the output power. It leads to the notably increasing of the total airgap flux as well. Thus, a necessity to have thicker back-iron parts leads to decreasing of the airgap diameter and, consequently, the output power.

It is obvious that the output power can be increased by rise of the armature current (or by increasing of the electrical loading) at the fixed magnet flux. It was shown in section V, the motor temperatures are near the given maximum limits, and the increasing of the electrical loading is not possible. This limitation could be overcome if the more efficient cooling system will be applied to the motor. For instance, the direct water cooling of the armature winding, instead of the water-jacket in the stator housing, could be a possible solution of this problem.

Other motor configurations, which are mentioned in section IV, have not been considered in this paper. Comparison of the designed SPM motor with those motor types and the possibilities of using those motors for the given application are treated in the second part of this paper (Part II).

ACKNOWLEDGEMENT

The authors gratefully thank Gemco-Trucks BV, the Netherlands for permission to publish the results of the common project.

REFERENCES

[1] J.R. Hendershot Jr. and T.J.E. Miller, *Design of brushless permanent magnet motors*,. Oxford, U.K.: Clarendon, 1994.
[2] W. Soong and T. J. E. Miller, "Field weakening performance of brushless synchronous AC motor drives," Proc. IEE—Elect. Power Appl., vol. 141, no. 6, pp. 331–340, Nov. 1994.
[3] EL-Refaie A.M., Jahns T.M., *Optimal Flux Weakening in Surface PM Machines Using Fractional-Slot Concentrated Windings*, IEEE Transaction on Industry Applications, vol. 41, no. 3, May/June 2005.
[4] Schiferl R.F.. Lipo T.A., *Power capability of salient pole permanent magnet synchronous motors in variable speed drive applications*, IEEE Transaction on Industry Applications, vol. 26, no. 1, Jan 1990.
[5] E. C. Lovelace, "Optimization of a magnetically saturable interior PM synchronous machine drive," Ph.D. dissertation, Dept. Elect. Eng. Comput. Sci., Massachusetts Inst. Technol., Cambridge, MA, 2000.
[6] E.V. Kazmin, J.J.H. Paulides, E.A. Lomonova, A.J.A. Vandenput, 'Motor re-ratings for traction applications', TUE report, 2007.
[7] A.V. Ivanov-Smolenskii.: *Electrical machines*, Energoatomizdat, Moscow, 1980. (in Russian)
[8] A.V. Ivanov-Smolensky, M.A. Avanesov, V.A. Martynov, "Calculation of the flux density harmonic components in the airgap of the electrical

machine with single slotted core", Electrichestvo, 7: 28-33, 1983 (in Russian).
[9] A.V. Ivanov-Smolenskii, Yu.V.Abramkin, A.I.Vlasov, V.A.Kuznetsov, "Universal Method of Electromagnetic Processes Calculation of Electric Machines", Moscow, "Energoatomizdat", 1986, p.216 (in Russian).
[10] F. Magnussen and C. Sadarangani, "Winding Factors and Joule Losses of Permanent Magnet Machines with Concentrated Windings",
[11] Flux 2D. Version 9.3. User's Guide
[12] Motor-CAD. Version 2.1. User's Manual